Structure of Supramers Formed by the Amphiphile Biotin-CMG-DOPE

Anton Zalygin,[a] Daria Solovyeva,[a] Ivan Vaskan,[a, f] Stephen Henry,[b] Marcel Schaefer,[b] Pavel Volynsky,[a] Alexander Tuzikov,[a] Elena Korchagina,[a] Ivan Ryzhov,[a] Alexey Nizovtsev,[a] Konstantin Mochalov,[a] Roman Efremov,[a, c] Eleonora Shtykova,[d, e] Vladimir Oleinikov,[a, f] and Nicolai Bovin*[a]

The synthetic function-spacer-lipid (FSL) amphiphile biotin-CMG-DOPE is widely used for delicate ligation of living cells with biotin residues under physiological conditions. Since this molecule has an "apolar-polar-hydrophobic" gemini structure, the supramolecular organization is expected to differ significantly from the classical micelle. Its organization is investigated with experimental methods and molecular dynamics simulations (MDS). Although the linear length of a single biotin-CMG-DOPE molecule is 9.5 nm, the size of the dominant supramer globule is only 14.6 nm. Investigations found that while the DOPE tails form a hydrophobic core, the polar CMG spacer folds back upon itself and predominantly places the biotin reside inside the globule or planar layer. MDS demonstrates that <10% of biotin residues on the highly water dispersible globules and only 1% of biotin residues in layer coatings are in an linear conformation and exposing biotin into the aqueous medium. This explains why in biotin-CMG-DOPE apolar biotin residues both in water dispersible globules and coatings on solid surfaces are still capable of interacting with streptavidin.

1. Introduction

Synthetic amphiphiles, so called function-spacer-lipid constructs (FSL),[1–3] were designed for insertion of biologically active small molecules into living cell membranes or for rapid coating of non-biological surfaces.[3] When the functional part is oligosaccharide, an artificial glyco-landscape is created,[1,3] although a large variety of small molecules can be used as an FSL function to modify biological and non-biological surfaces.[1–3] One particular molecule of this class is biotin-CMG-DOPE (Figure 1), which is able to attach biotin onto cells and surfaces and serve as a universal bridge for rapid and delicate modification of living cells with a variety of (strept)avidinylated molecules in physiological conditions.[2] Because amidated biotin (without its polar $-COO^-$ group) is a rather hydrophobic residue, it is insoluble in water when directly conjugated to DOPE. Therefore a highly polar CMG spacer (Figure 1) was designed to confer good dispersibility in water of biotin linked to DOPE.

Like any amphiphile, biot-CMG-DOPE must form micelle-like supramers in an aqueous environment, but because of the unusual "apolar-polar-hydrophobic" structure (that is, the asymmetric "gemini" amphiphile) we expected that supramolecular organization of this molecule will be signifi-

[a] A. Zalygin, D. Solovyeva, I. Vaskan, Dr. P. Volynsky, Dr. A. Tuzikov, Dr. E. Korchagina, Dr. I. Ryzhov, Dr. A. Nizovtsev, Dr. K. Mochalov, Prof. R. Efremov, Dr. V. Oleinikov, Prof. N. Bovin
Shemyakin-Ovchinnikov Institute of Bioorganic Chemistry
Russian Academy of Sciences
16/10 Miklukho-Maklaya str.
Moscow, 117997 (Russia)
E-mail: professorbovin@yandex.ru

[b] Dr. S. Henry, Dr. M. Schaefer
School of Engineering, Computer & Mathematical Sciences
Auckland University of Technology
Auckland 1010 (New Zealand)

[c] Prof. R. Efremov
National Research University Higher School of Economics, Myasnitskaya Str. 20, Moscow, 101000, Russian Federation

[d] Dr. E. Shtykova
Shubnikov Institute of Crystallography of Federal Scientific Research Centre 'Crystallography and Photonics' of Russian Academy of Sciences, Moscow 119333, Russian Federation

[e] Dr. E. Shtykova
Semenov Institute of Chemical Physics, Russian Academy of Sciences, Moscow 119991, Russian Federation

[f] I. Vaskan, Dr. V. Oleinikov
National Research Nuclear University MEPhI (Moscow Engineering Physics Institute), Kashirskoe shosse 31, Moscow, 115409, Russian Federation
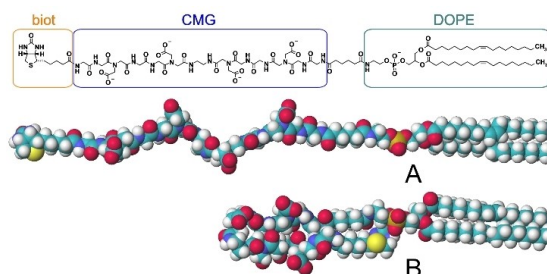
Figure 1. Structure of biot-CMG-DOPE; DOPE is 1,2-O-dioleoyl-*sn*-glycero-3-phosphatidyl ethanolamine; CMG is repeating glycyl-glycyl-N-carboxymethylglycyl motif; biot is 5-[(3aS,4S,6aR)-2-oxohexahydro-1H-thieno[3,4-d]imidazol-4-yl]pentanoyl moiety. A and B, the molecule in extended and (~9.5 nm) folded (~5.8 nm) conformations correspondingly.

ChemistryOpen

Full Papers
doi.org/10.1002/open.201900276

Chemistry Europe
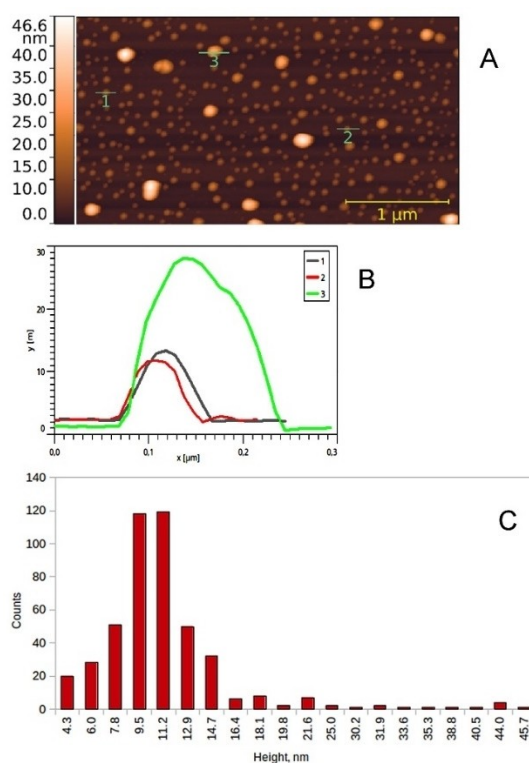European Chemical
Societies Publishing

cantly different from the canonical micelle. In this work, we investigated the organization of supramers formed by this gemini-amphiphile, with modern structural methods and molecular dynamics simulations. The data obtained for the globular particles explained why the biotin residue, which is apolar (and therefore expected to be associating with the lipid layer), is capable of interacting with streptavidin when biot-CMG-DOPE is present as a membrane-like layer on a surface.

2. Results

2.1. Characterization of the Size and Shape of Supramers by Experimental Physical Methods

Critical micelle concentration (CMC) value for biot-CMG-DOPE found to be 13 ± 0.7 μM and 50 ± 3.8 μM for PBS and water, respectively (Supplementary Figure S1 and a legend with experimental conditions and description of the method used).

Atomic force microscopy (AFM) was used to evaluate the shape, size and size distribution of the biot-CMG-DOPE supramers. The AFM image (Figure 2) shows ellipsoidal particles with a size range of 9–45 nm in height and 100–200 nm laterally. It is well known that in AFM due to the large radius of the scanning tip, a broadening in lateral size takes place. For this reason, we

used AFM only for estimation of general shape, and measurement of heights, while ignoring data on lateral sizes. Figure 2 shows the particle height distribution; the majority of particles have height ~10 nm, i.e. close to typical micelle size, while particles > 20 nm (supposedly aggregates) are low in number.

In an experiment using transmission electron microscopy (TEM), a biot-CMG-DOPE solution was applied and dried on the surface of a standard copper grid coated with a thin carbon film, then the surface was negatively contrasted with a 2% solution of uranyl acetate and washed to remove the poorly adhered material; a concentration of 0.2 mM was chosen in accordance with the CMC value (13 μM, see above). TEM demonstrates (Figure 3) globules with a nearly uniform spherical shape and a size of 11.5 ± 0.5 nm.

To avoid distortion due to drying or surface effects, measurements in an aqueous media were performed using dynamic light scattering (DSL). DLS showed a presence of two very distinct fractions (Figure S2). The predominant (> 95%) one was in the range of 9.5–15.3 nm interval (peak ~12 nm), and the minor (~1%) fraction, apparently, is an aggregated (120–300 nm) material. A slightly larger upper diameter value compared to AFM and TEM probably reflects the fact that DLS measures the hydrodynamic size, i.e. it also takes into account the solvating layer.

For in-depth structural analysis of the supramers formed by biot-CMG-DOPE molecules, we performed small angle X-ray scattering (SAXS) measurements at a concentration of 2.25 mM - higher than the CMC value. SAXS curves of biot-CMG-DOPE in a sodium phosphate buffer at pH 7.4 and pH 8.0 were found to be practically identical (Figure S3). Both scattering curves reveal noticeable upturns at very small angles, in the range of the scattering vectors $s < 0.25$ nm^{-1}. These results indicate that monodisperse ~14 nm biot-CMG-DOPE particles co-exist in solution with a moderate number of large assemblies. This observation correlates well with the AFM data (Figure 2) and DLS (Figure S2). It should be noted that the SAXS profiles are characteristic for scattering from micelle-like globules. Since large aggregates consisting of several globules contribute mostly to the results at the very small angles, discarding this portion of the data diminishes the influence of these particles when determining the shape of the practically monodisperse globules formed by the biot-CMG-DOPE molecules. Thus, the region $s > 0.25$ nm^{-1} can be used to calculate the distance
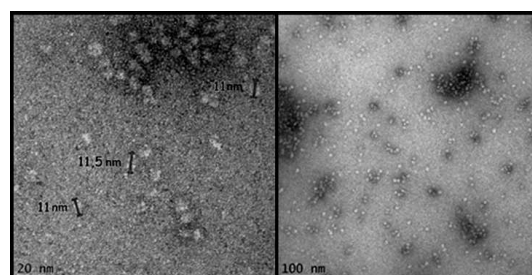
Figure 2. AFM image of biot-CMG-DOPE (A), corresponding height profiles (B; profiles 1 (gray line) and 2 (red line) correspond to the small particles in the panel A, profile 3 (green line) is the result of the particles overlapping and aggregation, as indicated by the double-triple size of large particles. The size distribution (C), shows the predominance of ~10 nm size particles. AFM conditions were, mica surface, in air, semi-contact mode, 10 nm radius of cantilever tip.

Figure 3. TEM of spherical particles formed by biot-CMG-DOPE. The left image allows estimation the shape of the particles, while the right image (5 times less magnification) demonstrates the uniformity in their size. Transmission electron microscope Zeiss Libra 120 (Germany).

ChemistryOpen

Full Papers
doi.org/10.1002/open.201900276

Chemistry
Europe
European Chemical
Societies Publishing

distribution function and to restore a shape of the supramer using the *ab initio* procedure (program DAMMIN). The result of the three-dimensional shape reconstruction is shown in Figure 4. The shell of the reconstructed structure (Figure 4b) is formed by the regions with high electron density corresponding to biotin residues and CMG motifs. Central "void" is associated with a low electron density of the DOPE lipid tails. The shape and the particle sizes of about 11–12 nm obtained by this method are generally consistent with the results of other used methods (see above).

2.2. Coarse-Grained MD Simulations

Since experimental methods (see above) only gave us size and shape of the particle, and an approximation of structural organization, we performed coarse-grained MDS of self-assembly of the globules.

The simulation was carried out with different concentrations of biot-CMG-DOPE, in all cases the evolution of the system was the same. In the first 10 ns of the MDS, biot-CMG-DOPE formed small micelle-like globules (Figure 5c) in contact with each other (Figure 5b). Cluster analysis showed that, regardless of the biot-CMG-DOPE concentration, all molecules aggregate into one cluster in the first 50 ns of MDS (Figure 5a). This cluster consists of globules contacting by their CMG motifs. After 200 ns, a dense cluster of globules forms (Figure 5d), where they are able to exchange individual molecules. Exchange is quite intense in the early stages of dynamics (see evolution of the distribution of globule sizes in the first 200 ns (Figure 5f), slowing down in the last stages of MDS (Figures 5b and 5 g). After 1 μs of dynamics, the system consists of several closely packed globules (more than 55 molecules each) (Figure 5e).

To study the molecular organization inside the particle, we randomly selected two representative globules of different sizes, placed them in a 15 nm box, and performed a 100 ns all-atoms simulation. The resulting structure is shown in Figure 6. The hydrophobic nucleus comprised of DOPE lipid tails, is surrounded by CMG residues, which are mostly folded back upon themselves causing most of the apolar biotin moieties to be internalized within the globule (the biotin moieties are easily located in the figure due to their yellow sulfur residues). The organization of globules of different sizes was similar.

This simulation suggests that at any one point in time the majority of apolar biotin residues are buried within the globule (80 to 90 % of sulfur grain had surface less than 1 nm^2), which allows the polar CMG residues to be surface facing and hence accounts for the high polar dispersibility of the globule. On the other hand, we observe (Figure 5h) that 10–15 % of biot-CMG-DOPE molecules has biotin exposed to water. The radius of the globule was determined as $r = (5/3)^{1/2} r_g$, where r_g is the radius of gyration, which was computed using GROMACS software. The r_g values of 3.16 nm and 3.50 nm obtained from the simulation lead to diameters of 8.16 nm and 9.0 nm. The difference in particle sizes between the experimental data (according to SAXS, the number of molecules in one globule lies in the range of 145–180) and MDS we explain by using the rough approximation model in the simulation; in particular, simplified electrostatic description was used.

Averaged conformation of single biot-CMG-DOPE molecule within the globule (Figure 6e) appears to be folded back upon itself at the relatively flexible -CH$_2$CH$_2$- region.
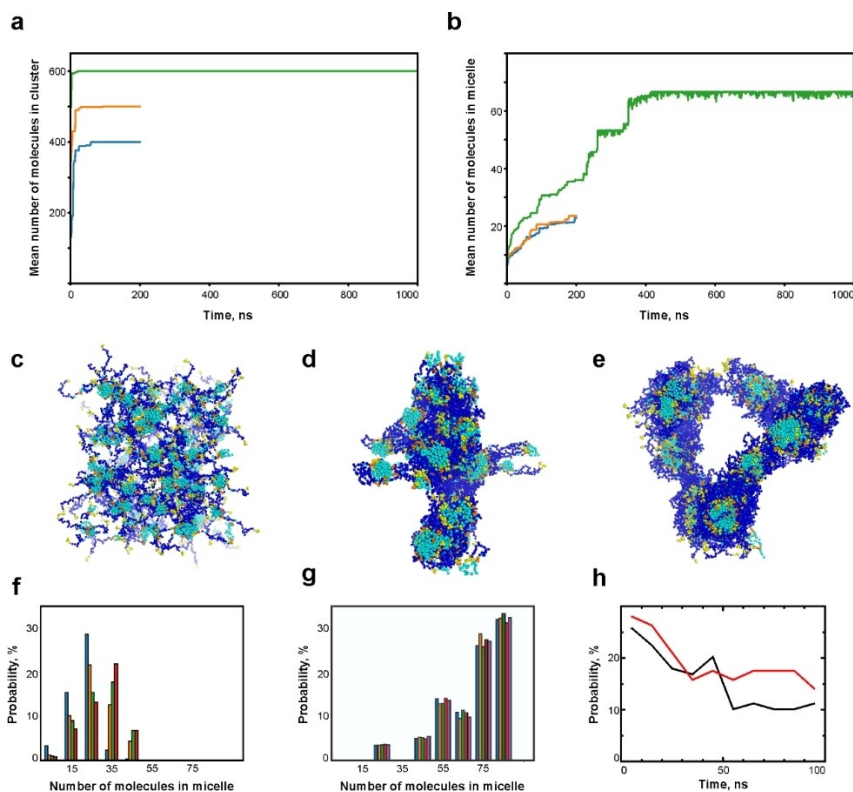
2.3. MDS of the Planar Layer

MD simulations of lipid bilayers consisting of biot-CMG-DOPE molecules were carried out in full-atom representation for two extreme conformation states – linear and folded (Figure 1, A and B). In the simulation with 200 biot-CMG-DOPE molecules in the linear state, the biot-CMG region of biot-CMG-DOPE molecules has a conformation where the biotin residues are all exposed to solvent; here, DOPE tails are well packed. In the folded state, biot-CMG fragment is folded in the middle of its CMG part at the relatively flexible region —CH$_2$—CH$_2$—, so that the biotin residue is located near the PO$_4$, and the group —(CH$_2$)$_4$— between phosphoethanolamine and CMG in the linker is in close proximity to the —(CH$_2$)$_4$— group belonging to biotin (Figure 7).

The study of these two, linear and folded, states was performed for the following reasons: (i) the structural organization of biot-CMG-DOPE molecules in flat layers is not known from experiments; (ii) large-scale conformational transitions between linear and folded conformations cannot be observed in the MDS even on a microsecond time(see below).
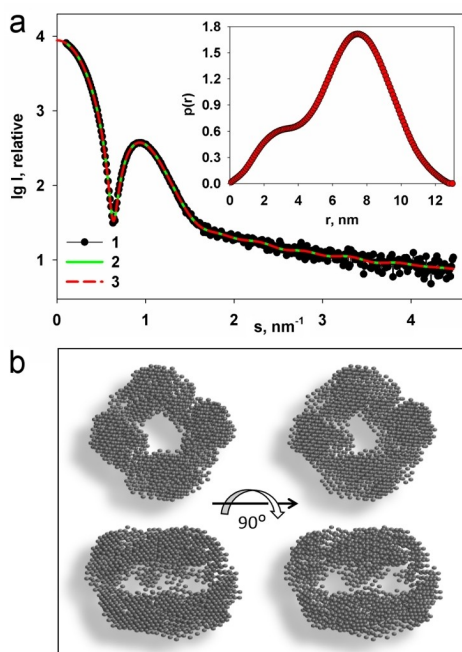
Figure 4. Shape restoration of the biot-CMG-DOPE globules. (a): SAXS data (1), scattering patterns computed from the *ab initio* model (2), transformed from *p(r)* and extrapolated to zero scattering angle intensity (3). Insert: distance distribution function *p(r)* computed by GNOM. (b): stereo image of structural model reconstructed by *ab initio* modeling. The apparent central "void" does not represent an absence of atoms, hydrocarbon nucleus is transparent to X-rays.

ChemistryOpen

Full Papers
doi.org/10.1002/open.201900276

Chemistry Europe
European Chemical
Societies Publishing

Figure 5. Evolution of the mean size of biot-CMG-DOPE globules calculated based on contacts of all (a) or tail atoms (b). Initial (t = 0, figure c) and final (t = 200 ns, figure d) structures obtained as a result of 200 ns MDS of 400 biot-CMG-DOPE molecules, and final structure obtained as a result of 1 μs MDS of 600 biot-CMG-DOPE molecules (t = 1 μs, figure e) structures. Water molecules, Na$^+$ and Cl$^-$ ions are omitted for clarity. Biotin residues are in yellow, CMG fragments are in blue, phosphate groups are in orange, hydrophobic fragments (mostly DOPE residues) are in cyan. (f, g) Distributions of biot-CMG-DOPE over the globule for time interval 0–200 ns (figure f) and 500–1000 ns (figure g) different colors correspond to the distribution at different time intervals. (h) A fraction of molecules biot-CMG-DOPE in which biotin is exposed at the globule periphery as a function of simulation time; the red and black curves correspond to small (57 molecules) and large (89 molecules) globules.

Therefore, to explore possible scenarios the two extreme conformations of linear and folded were examined. When folded, the CMG fragment has a cross section of double area compared to the linear state, but a half length. In the folded state the biotin residue is hidden and therefore does not interact with solvent. Simulation details are presented in Table S1. When analyzing bilayers, we considered the following: 1) the bilayer parameters (thickness, area per DOPE residue); 2) density profiles of biotin, phosphate, DOPE residues and water; 3) the accessible surface area of the biotin residue; 4) intra- and intermolecular hydrogen bonds in biot-CMG-DOPE.
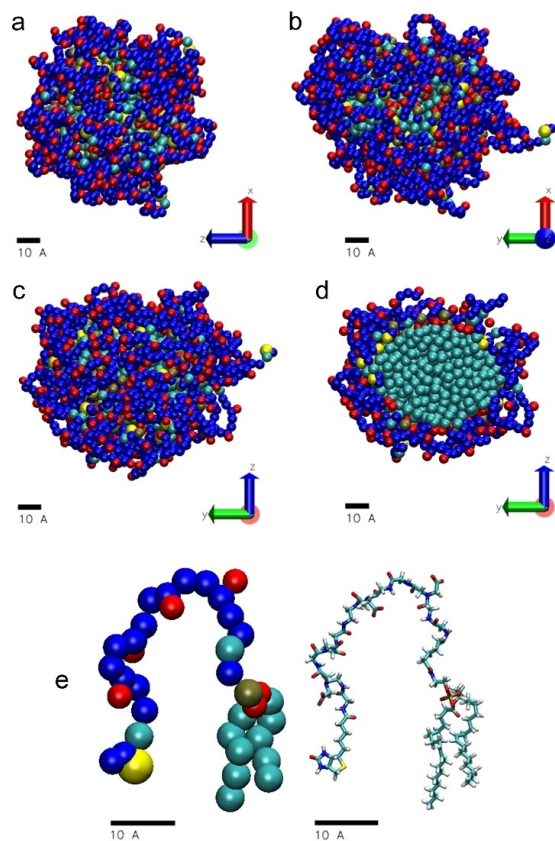
A detailed analysis is presented in Supplementary Section S5; in brief, the results are as follows. Bilayers consisting of biot-CMG-DOPE molecules are stable in the microsecond range in both states - with linear and folded CMG fragment (as well as in their "mixed" system). Transitions between the later are hampered by the need to break ~3 hydrogen bonds (in the folded state) and transfer biotin through a dense region of the highly polar CMG. The appearance in the bilayer of a limited number of linear biot-CMG-DOPE molecules (having a rigid elongated conformation) potentially hinders the deployment of other linear molecules since the corresponding lipid part becomes more densely packed. This, in turn, increases the path

length for releasing the biotin residue from its crypted position to a linear state accessible to the solvent.

When the MDS starts from a state, where biot-CMG fragments are folded, about 1% of the biotin moieties are in a linear state and potentially available for interaction with streptavidin. An increase in temperature from 310 to 350 K during simulation leads to an increase in the number of the linear structures potentially accessible to streptavidin. On the other hand, the total population (in %) of such linear molecules falls because these states become short-lived.

2.4. AFM of Biot-CMG-DOPE Monolayer

For estimation the layer thickness on a flat surface, a silicon wafer chip polished to a roughness of 2 nm was used. We did not use regular AFM substrate, mica, to avoid the expected effect of negatively charges mica on the conformation of the negatively charged CMG fragment of biot-CMG-DOPE. The results (Figure S6) indicate a film thickness of ~7 nm, which is closer to the folded conformation of the molecule, which equates to 5.8 nm, than to its unfolded (9.5 nm) version.

ChemistryOpen

Full Papers
doi.org/10.1002/open.201900276

Chemistry Europe
European Chemical
Societies Publishing

Figure 6. Molecular Dynamics Simulation of the biot-CMG-DOPE supramer, in three projections: (a) ZX plane, (b) YX plane, (c) YZ plane; and (d) as a cross-section of (c); (e) average conformation of single molecule when present in a micelle-like supramer: left, coarse-grained molecular, right, all-atom model retrieved from the coarse-grained one using VMD software.[7] Biotin residues are in yellow, CMG fragments are in blue (carboxyl groups are in red), phosphate groups are in tan, hydrophobic fragments (mostly DOPE residues) are in pale-blue.

3. Discussion

The presence of two different lipophilic sites in the amphiphilic biot-CMG-DOPE molecule (Figure 1) suggests the potential for usual or atypical conformations in aqueous environments. Furthermore, the presence of a flexible hinge $-CH_2CH_2-$ region separating the two rigid halves of the CMG spacer, in principle allowing the hydrophilic CMG to adopt different conformations, further increases the potential for a variety of conformations. With this in mind, we investigated biot-CMG-DOPE with a variety of methodologies.

The experimental data consistently led to the conclusion that biot-CMG-DOPE in solution adopts one preferred architecture, micelle-like globules with a diameter of about 12–15 nm. However, the fully elongated biot-CMG-DOPE molecule has a length of 9.5 nm (Figure 1A), which clearly implies that the molecule in the micelle-like globule does not exist in a typical linear end-to-end state but must adopt some other conformation. Because the CMG motif has a flexible hinge region, the biot-CMG-DOPE molecule is able to adopt a folded state with a length of 5.8 nm, a state which also aligns the two apolar regions (DOPE and biotin). As shown in Figure 1B & 6e, such a conformation not only reduces the size of the globule but also presents a net hydrophilic surface to the outside of the globule, thereby supporting a high level of its dispersibility in water. However, the two negatively charged "halves" of CMG fragment are adjacent to each other, which may be disadvantageous due to electrostatic reasons, or is advantageous due to the formation of hydrogen bonds. Judging by the fact that pH does not affect the architecture of particles (SAXS experiment, Figure S3), there is no electrostatic repulsion or it is insignificant (e.g., because of solvation effect). It could be expected that there is a conformation (or their family) being the middle between these two extreme ones, that is, the molecule bends along the $-CH_2CH_2-$ hinge, but $-COOH$ groups of the same
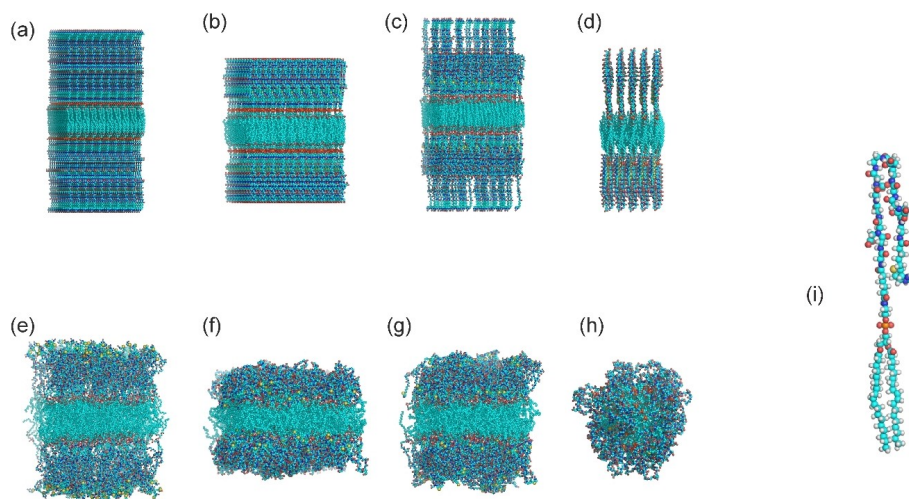

Figure 7. MD simulation of biot-CMG-DOPE in the composition of bilayers and a globule: a & e, 100% of the extended St-1 conformation before and after the dynamics; b & f, 100% folded St-2 conformation; c & g, 50% of extended and 50% of folded conformations; d & h, a globule composed of 60 biot-CMG-DOPE molecules in the folded St-2 conformation; i, conformation of a single folded molecule in the composition of St-2. In contrast to averaged folded conformation in the globule (Figure 6e), the flat layer is more tightly packed, and therefore the contact between the two $-(CH_2)_4-$ motifs became favorable, despite the low enthalpy of this interaction. Biot residues are highlighted by their yellow sulfur atoms.

ChemistryOpen

Full Papers
doi.org/10.1002/open.201900276

**Chemistry
Europe**
European Chemical
Societies Publishing

CMG chain do not converge; then, the individual molecule biot-CMG-DOPE loses the gain from approaching two —(CH$_2$)$_4$—, but in the supramer, a favorite contact between biot and DOPE residues belonging to different molecules (Figure 6d) can occur.

MD simulations confirm the preference for this "averaged" conformation in the particle composition (Figure 6e). Thus, the biot-CMG-DOPE amphiphile forms a micelle-like globule, in which the DOPE tails are surrounded by CMG while the biotin residues are tucked within the core although some of them (presumably, < 10%) are located on the periphery and available for interaction with streptavidin (Figure 6). One would expect the dynamic range between folded and unfolded structures could be able to be controlled to some extent by external factors such as temperature, and this is supported by MDS, which showed an increase in unfolded state with an increase in temperature.

The partial exposure of apolar biotin groups at the periphery of the globule explains the observed aggregation by DLS (Figure S2). This solution-phase model of a micelle-like globule agrees well with the experimental data, but cannot be transferred to surface coatings on hydrophobic or hydrophilic materials.[2] Therefore, we studied the planar surface coating layers using AFM and MDS. A layer thickness of ~7 nm (AFM data, Figure S6) indicates that biot-CMG-DOPE forms a layer of molecules existing on a neutral surface in a folded conformation rather than a bilayer or a monolayer in an expanded conformation, or densely packed globules. MDS showed that in the monolayer only about 1% of the biotin-CMG-DOPE molecules will exist on a surface if one assumes their unfolded state. This 1% corresponds to one available biotin residue per a square of 10×10 molecules, that is, a reactive residue within a diameter of ~10 nm. Given that the diameter of the streptavidin molecule is ~7 nm, then almost complete coverage of a surface with this protein can be expected. This fortuities and modest rate of biotin presentation probably explains why biot-CMG-DOPE has proved to be a good reagent for biotinylation of surfaces.[2] Not only is the biotin residue presented in a good format for reactivity with streptavidin, but the surface is also predominantly polar (due to CMG) a state conducive to good interactions with biological solutions and proteins. Conversely, if all or most of the biotin residues were all presented at the surface then not only would there be steric hindrance of the relatively bulky streptavidin, but also the surface would be apolar. It remains unclear, how the actual mechanism works in reality: whether there is a permanent presence of about 1% of biotin residues, or whether there is a dynamic "pop-up" process (Figure 8), with the potential to be controlled. Finally, it should be noted that the presentation of biotin-CMG-DOPE in cell membranes will also be different to surface coatings. In this setting, the lipid tail is inserted into the lipid membrane, and more likely resembles the micelle environment, albeit with the molecules diffusely spread throughout the cell membrane. The consequences and effects of the flexible spacer and the potential for "pop-up" residues in cell membranes remain unknown at this time.
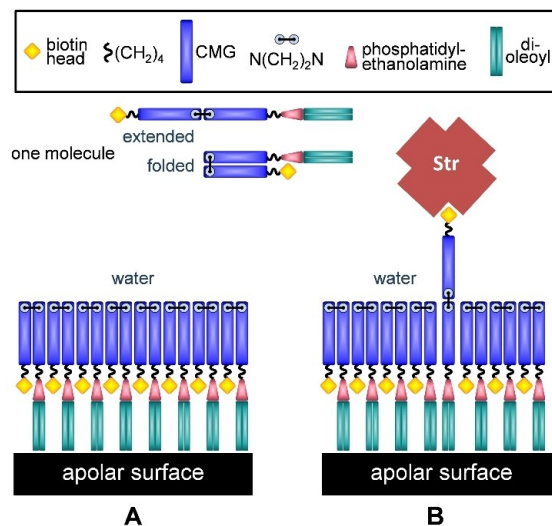
Figure 8. Predicted schematic of biot-CMG-DOPE coating of surfaces. A, monolayer on apolar surfaces; B, a pop-up of unfolded molecule and its binding to streptavidin.

Experimental Section

The following concentrations of biot-CMG-DOPE were used: AFM, 100 μM; TEM, 200 μM; DLS, 100 μM; SAXS, 2.25 mM.

Materials

All salts, solvents, lipids and other chemicals were from Sigma (St. Louis, USA).

Synthesis of biot-CMG-DOPE is described.[2]

Atomic Force Microscopy (AFM)

For AFM imaging of a globular form of biot-CMG-DOPE, the sample solution was diluted to an appropriate concentration (100 μM) with PBS buffer (pH 7.4). The sample (10 μl) was deposited onto a freshly cleaved mica surface. After 15 min incubation at room temperature, the mica was rinsed three times with 100 μl Milli-Q water in order to remove salts and unbound material, followed by drying in desiccator for 24 hours. After that, the sample was loaded for AFM imaging. AFM images were obtained at 25 °C and a relative humidity 35%. Atomic force microscope SFC113LNTF (NT-MDT, Russia) with silicon probes HA_HR/50 (NT-MDT, Russia) with resonance frequency 230 kHz were used. The scan rate was 0.78 Hz and the scan size was typically 5 μm. AFM was operated in the tapping mode. Sample imaging and height measurements were done using Nova software (NT-MDT, Russia).

For AFM imaging of a monolayer form of biot-CMG-DOPE, a WITech alpha300 RA system (ULM, Germany) was utilised with an AFM Arrow Cantilever, stiffness is 0.2 N/m, in the tapping mode. To determine the layer thickness, a scan of the surface topography was performed, and a part of the coated and a part of the removed material was captured within an area scan of 10 μm by 10 μm.

Transmission Electron Microscopy (TEM)

Transmission electron microscopy was carried out at conc. of biot-CMG-DOPE 200 μM in a phosphate buffer, pH 7.4; the solution was applied at copper grid coated with a thin carbon film; in 20 min the

ChemistryOpen

Full Papers
doi.org/10.1002/open.201900276

Chemistry Europe
European Chemical
Societies Publishing

adsorbed material was negatively contrasted with a 2% solution of uranyl acetate. The not adsorbed material was removed from the surface in a weak current of distilled water.

Dynamic Light Scattering (DLS)

Data on size and size distribution were obtained by dynamic light scattering. All measurements were performed on a Brookhaven Instruments 90Plus particle size analyzer (Brookhaven Instruments Corporation, USA). Sample solution (2 ml, 100 μM) in PBS buffer (pH 7.4) was sonicated for 15 s, and in 10 min measurements were taken during 30 sec at room temperature.

Small Angle X-ray Scattering (SAXS)

Synchrotron SAXS measurements were performed at the European Molecular Biology Laboratory (EMBL) on the storage ring PETRA III (DESY, Hamburg) at the EMBL-P12 beam line equipped with a robotic sample changer and a 2D photon counting pixel X-ray detector PILATUS-2M (DECTRIS, Switzerland). The scattering intensity, $I(s)$, was recorded in the range of momentum transfer $0.05 < s < 5.0$ nm^{-1}, where $s = (4\pi \sin\theta)/\lambda$, 2θ is the scattering angle, and $\lambda = 0.124$ nm is the X-ray wavelength.[7]

The measurements were performed at the biot-CMG-DOPE concentration 2.25 mM in a sodium phosphate buffer, pH 7.4 and 8.0, at 22 °C using continuous flow operation over a total exposure time of 1 s collected as 20×50 ms individual frames to monitor for potential radiation damage (no radiation effects were detected).[8] The data were corrected for the solvent scattering and processed using standard procedures[11] with additional data analysis performed using the program PRIMUS.[12] Distance distribution function $p(r)$ and the maximal diameter of the particle, D_{max}, were evaluated by the program GNOM[13] using Equation (1).

$$p(r) = \frac{1}{2\pi^2} \int_0^\infty srI(s)\sin(sr)ds \qquad (1)$$

The low-resolution shapes were reconstructed by the *ab initio* method, DAMMIN,[14] employing a dummy atom (bead) model of the particle. Starting from a random assembly, the program utilizes simulated annealing (SA) to build models fitting the experimental data, $I_{exp}(s)$, with minimal discrepancy.

$$\chi^2 = \frac{1}{N-1} \sum_j \left[\frac{I_{exp}(s_j) - cI_{calc}(s_j)}{\sigma(s_j)} \right]^2 \qquad (2)$$

where N is the number of experimental points, c is the scaling factor and $I_{calc}(s_j)$ and $\sigma(s_j)$ are the calculated intensity from the model and the experimental error at the momentum transfer, s_j, respectively, Equation (2).

Multiple *ab initio* reconstructions were performed to obtain consistent models. The DAMMIN outputs were analyzed using programs SUPCOMB[15] and DAMAVER[16] to identify the most typical models of the specimen.

Molecular dynamics simulations (MDS).

Molecular dynamic was carried out using GROMACS package version 2016.1.[16] To analyze the aggregation of biot-CMG-DOPE molecules in water, we used coarse-grained approximation. To this end, 400, 500 and 600 molecules were placed in a rectangular box (20×20×20 nm³) in random orientation. Then the system was solvated and some ions Na$^+$ and Cl$^-$ were added in such a way that the system had a zero total charge and an ionic strength of 0.15 M. Then system was equilibrated at 10 ns MD run at constant pressure (1 bar, Berendsen barostat[17]) and temperature (300 K, Nose-Hoover thermostat). Finally, 200 ns MDS at a constant volume and temperature 300 K was performed. In order to better analyze the self-assembly of biot-CMG-DOPE molecules, the duration of the calculation in the 600 molecules system was increased to 1 μs. Coarse-grained molecular models (details are provided in Supplementary Section S4) were created using PyCGTOOL software.[4] The assembling of atoms was carried out as in.[4] In this model, the negative charge corresponds to the protonation state of the molecule at pH 7. The aggregation of biot-CMG-DOPE molecules was studied using home-made software. Lipids were considered to belong to the same cluster if the grains were in contact with any atoms at a distance of less than 0.6 nm. To analyze the behavior of globules in solution, we selected two of them with different sizes and made 100 ns MDS in aqueous solution with a similar modeling protocol.

Then, the behavior of biot-CMG-DOPE in the layers and the refinement of the properties of globules were carried out in the full-atom approximation. In the simulation, we used the Slipids-based parametrization[18] of lipid molecules and the TIP3P model of water. Molecular parameters, the system construction and the simulation were similar to described in.[19] In total, four 1 μs simulations were performed: three simulations of bilayers composed of biot-CMG-DOPE with different conformation of the biot-CMG motif, and one simulation of globules consisting of 60 molecules based on the behavior in the coarse-grained representation (see above). Other modeling details are provided in the Supporting Information.

4. Conclusions

Biotin-CMG-DOPE serves as a universal bridge for the rapid and delicate modification of living cells with biotin and various (strept)avidinylated molecules under physiological conditions.[2] For example, the red blood cells biotinylated with biotin-CMG-DOPE were extracted using their biotin residue from blood after having been in the circulation for 24 hours,[14] which opens up horizons for therapeutic *in vivo* technologies based on the modification of cells with biotin-CMG-DOPE. As a consequence, it is important to understand the supramolecular organization of this molecule in the composition of the cell membrane, and also its potential ability to "hide" its biotin residues from biotin-destroying blood enzyme[15] and biotin-specific natural antibodies,[16] while still leaving biotin available for interaction with avidin.[14]

ChemistryOpen

Full Papers
doi.org/10.1002/open.201900276

Chemistry Europe
European Chemical
Societies Publishing

Conflict of Interest

The authors declare no conflict of interest.

Keywords: amphiphiles · function-spacer-lipid · biotin · molecular dynamics · supramers · molecular dynamics simulations

[1] E. Y. Korchagina, S. M. Henry, *Biochemistry (Moscow),* **2015**, *80*, 857–871. DOI: 10.1134/S0006297915070068.

[2] S. Henry, E. Williams, K. Barr, E. Korchagina, A. Tuzikov, N. Ilyushina, S. A. Abayzeed, K. F. Webb, N. Bovin, *Sci. Rep.*, **2018**, *8* 2845. DOI:10.1038/s41598-018-21186-3, SREP-17-08556-2.

[3] E. Williams, K. Barr, E. Korchagina, A. Tuzikov, S. Henry, N. Bovin, *Int. J. Mol. Sci.*, **2016**, *17*, 118. DOI: 10.3390/ijms17010118.

[4] J. A. Graham, J. W. Essex, S. Khalid, *J. Chem. Inf. Model.*, **2017**, *57*, 650–656.

[5] W. Humphrey, A. Dalke, K. Schulten, *J. Mol. Graphics*, **1996**, *14*, 33–38.

[6] C. E. Blanchet, A. Spilotros, F. Schwemmer, M. A. Graewert, A. G. Kikhney, C. M. Jeffries, D. Franke, D. Mark, R. Zengerle, F. Cipriani, S. Fiedler, M. Roessle, D. I. Svergun, *J. Appl. Crystallogr.*, **2015**, *48*,431–443.

[7] C. M. Jeffries, M. A. Graewert, D.I Svergun, C. E. Blanchet, *J. Synchrotron Radiat.*, **2015**, *22*, 273–279.

[8] D. Franke, M. V. Petoukhov, P. V. Konarev, A. Panjkovich, A. Tuukkanen, H. D. T. Mertens, A. G. Kikhney, N. R. Hajizadeh, J. M. Franklin, C. M. Jeffries, D. I. Svergun, *J. Appl. Crystallogr.*, **2017**, *50*: 1212–1225.

[9] P. V. Konarev, V. V. Volkov, A. V. Sokolova, M. H.J Koch, D. I. Svergun, *J. Appl. Crystallogr.*, **2003**, *36*, 1277–1282.

[10] D. I. Svergun, *J. Appl. Crystallogr.*, **1992**, *25*, 495–505.

[11] D. I. Svergun, *Biophys. J.*, **1999**, *76*, 2879–2886.

[12] M. V. Kozin, D. I. Svergun, *J. Appl. Crystallogr.*, **2001**, *34*, 33–41.

[13] V. V. Volkov, D. I. Svergun, *J. Appl. Crystallogr.*, **2003**, *36*, 860–864.

[14] C. Oliver, D. Blake, S. Henry, *Transfusion*,**2011**,*51*, 1723–1730.

[15] J. Chauhan, K. Daskhinamur, *J. Biol. Chem.*, **1986**, *261*, 4268–4275.

[16] M. J. Abraham, T. Murtola, R. Schulz, S. Pall, J. C. Smith, B. Hess, E. Lindahl, *SoftwareX*, **2015**, *1–2*, 19–25.

[17] H. J. C. Berendsen, J. P. M. Postma, W. F. van Gunsteren, A. DiNola, J. R. Haak, *J. Chem. Phys.,* **1984**, *81*, 3684–3690.

[18] I. Ermilova, A. P. Lyubartsev, *J. Phys. Chem. B*, **2016**, *120* (50), 12826–12842.

[19] P. Volynsky, R. Efremov, I. Mikhalev, K. Dobrochaeva, A. Tuzikov, E. Korchagina, P. Obukhova, E. Rapoport, N. Bovin, *Mol. Immunol.*, **2017**, *90*, 87–97.